Automated blood vessel extraction using local features on retinal images

Yuji Hatanaka*[a], Kazuki Samo[b], Mikiya Tajima[b], Kazunori Ogohara[a], Chisako Muramatsu[c], Susumu Okumura[d], Hiroshi Fujita[c]

[a]Department of Electronic Systems Engineering, School of Engineering, the University of Shiga Prefecture, 2500 Hassaka-cho, Hikone, Shiga, Japan 522-8533;
[b]Division of Electronic Systems Engineering, Graduate School of Engineering, the University of Shiga Prefecture, 2500 Hassaka-cho, Hikone, Shiga, Japan 522-8533;
[c]Department of Intelligent Image Information, Division of Regeneration and Advanced Medical Sciences, Graduate School of Medicine, Gifu University, 1-1 Yanagido, Gifu, Japan 501-1194;
[d]Department of Mechanical Systems Engineering, School of Engineering, the University of Shiga Prefecture, 2500 Hassaka-cho, Hikone, Shiga, Japan 522-8533

ABSTRACT

An automated blood vessel extraction using high-order local autocorrelation (HLAC) on retinal images is presented. Although many blood vessel extraction methods based on contrast have been proposed, a technique based on the relation of neighbor pixels has not been published. HLAC features are shift-invariant; therefore, we applied HLAC features to retinal images. However, HLAC features are weak to turned image, thus a method was improved by the addition of HLAC features to a polar transformed image. The blood vessels were classified using an artificial neural network (ANN) with HLAC features using 105 mask patterns as input. To improve performance, the second ANN (ANN2) was constructed by using the green component of the color retinal image and the four output values of ANN, Gabor filter, double-ring filter and black-top-hat transformation. The retinal images used in this study were obtained from the "Digital Retinal Images for Vessel Extraction" (DRIVE) database. The ANN using HLAC output apparent white values in the blood vessel regions and could also extract blood vessels with low contrast. The outputs were evaluated using the area under the curve (AUC) based on receiver operating characteristics (ROC) analysis. The AUC of ANN2 was 0.960 as a result of our study. The result can be used for the quantitative analysis of the blood vessels.

Keywords: Blood vessel extraction, Local feature, High-order local autocorrelation, Hypertensive retinopathy, Arteriolar narrowing, CAD, Retinal image, Segmentation

1. INTRODUCTION

Funduscopy is useful for early detection of diabetic retinopathy, hypertensive changes, arteriosclerotic changes, and glaucoma. Retinas are examined using retinal images. In most cases, ophthalmologists or physicians use the Scheie classification based on the condition of blood vessels. Hypertensive retinopathy is graded by the diameter ratio of arteries and veins, hemorrhages, and exudates. However, human observation does not provide quantitative results. Thus, many blood vessel extraction methods have been proposed [1–18].

Tolias et al. proposed a vessel and nonvessel region classification method using a fuzzy c-means clustering algorithm [1]. Niemeijer et al. proposed a segmentation method based on Gaussian matched filter and kNN [2]. Soares et al. proposed a segmentation method based on a feature vector composed of pixel intensity and two-dimensional Gabor wavelet transform responses taken at multiple scales [3]. Rangayyan et al. proposed a method that used a bank of directionally sensitive Gabor filters (GF) with tunable scale and elongation parameters [4]. Kharghanian et al. proposed a method based on seven features; a feature using pixel intensity, four features from Gabor wavelet transform in different scales, and two features from orthogonal line operators [5]. Miri et al. proposed a method based on image enhancement

*hatanaka.y@usp.ac.jp; phone 81 749 28-9556; fax 81 749 28-9576

Medical Imaging 2016: Computer-Aided Diagnosis, edited by Georgia D. Tourassi, Samuel G. Armato III,
Proc. of SPIE Vol. 9785, 97852F · © 2016 SPIE · CCC code: 1605-7422/16/$18 · doi: 10.1117/12.2216572

using a curvelet transform that represents edges [6]. Chaudhuri et al. proposed a method using matched filters [7]. Ricci et al. applied a line detector, which has been previously used in mammography [8]. Yu et al. proposed a method based on a multiscale active contour model using eigenvalues of local second order derivatives (Hessian matrix) [9]. Staal et al. proposed a method based on image ridge extraction using a kNN-classifier with properties of the patches and line elements [10]. Salem et al. suggested a method using a clustering algorithm with a partial supervision strategy [11]. They showed that their method could segment blood vessels with small diameters and low contrast. Paripurana et al. proposed a method using background estimation calculated using a weight surface fitting method with a high degree polynomial [12]. Zana et al. proposed a method based on morphological filter and cross-curvature [13]. For segmentation of the optic cup region, we proposed a method using gradient vector concentration [14]. We also proposed a method using a double-ring (DR) filter, which can work quickly [15]. The DR filter calculates the mean difference in the inner circle and outer ring regions. We proposed a method using a black top-hat (BTH) transformation [16], and we developed a method based on BTH combined with DR filter [17]. However, previously proposed method [17] returned suboptimal segmentation accuracy of major arteries, especially those with low contrast and central reflex. To improve the recognition rate of major vessel pairs, synthetic vessel models were created, and the missed or broken arteries were identified by template matching [18]. However, creating an optimal synthetic vessel model is too difficult for practical application.

To the best of our knowledge, a blood vessel extraction method based on the relation of neighbor pixels has not been proposed. Determining parameters, such as optimal filter size and shape, is difficult. Ohtsu et al. proposed the use of high-order local autocorrelation (HLAC) features as the primitive image features [19]. HLAC is effective for many image recognition applications [20–22]. HLAC has demonstrated high performance in a facial recognition study [20], a chest nodule detection study [21], and a human sensing study using microwave Doppler radar [22]. HLAC features are shift-invariant and model-free. HLAC is appropriate for center-shifted hotspot pattern feature extraction. A general template-matching technique depends strongly on a preset model. Patterns of blood vessels are so varied that designing a flexible blood vessel model is not practical. However, HLAC does not require a preset model. Thus, HLAC is expected to be effective for blood vessel extraction. This paper describes blood vessel extraction based on HLAC and presents the results for HLAC and previous simple methods that do not rely on complicated algorithms.

2. METHODS

2.1 HLAC

We apply HLAC [19] as the feature of blood vessels. The *N*-th order HLAC is calculated by the following autocorrelations:

$$R_N^T(a_1, a_2, \dots, a_N) = \sum_r I(r)I(r + a_1) \dots I(r + a_N) \quad (1)$$

where $I(r)$ is a pixel value of the image, T is the local pattern number, $r = (x, y)'$ (the dash denotes the transpose) is position vector a, a_i are the displacement vectors, and x and y are coordinates in the image. By varying the parameter values a and N, (1) can take many forms; therefore, N was limited to ($N = 0, 1, 2$). The range of displacements was also limited to within a local 3 × 3 window, whose center was the position of interest. By reducing the displacements, which are equivalent by the shift, T was limited to 35 ($T = 1, 2 \dots 35$). The 35 kinds of general patterns are shown in Figure 1. In this study, window size was expanded to 5 × 5 and 7 × 7 (as shown in Figure 1 (b)), and 105 HLAC patterns (35 patterns per window size) were applied to extract the blood vessels.

Initially, we considered calculating HLAC features in the region of interest (ROI). However, HLAC has directional dependency. For example, the HLAC features of two blood vessel models, as shown in Figure 2(b) and 2(c), differ. Thus, we transformed the ROI to a polar coordinate image (Figure 2(a)) and calculated the HLAC. The HLAC features of two polar-transformation images (Figure 2(d) and 2(e)) were similar. Thus, HLAC features with polar transformation are considered turn-invariant.

2.2 Extraction of blood vessels based on HLAC features

Image database

The retinal images used in this study were obtained from the "Digital Retinal Images for Vessel Extraction" (DRIVE) database [10]. The database includes 40 retinal fundus images that were obtained from a diabetic retinopathy screening

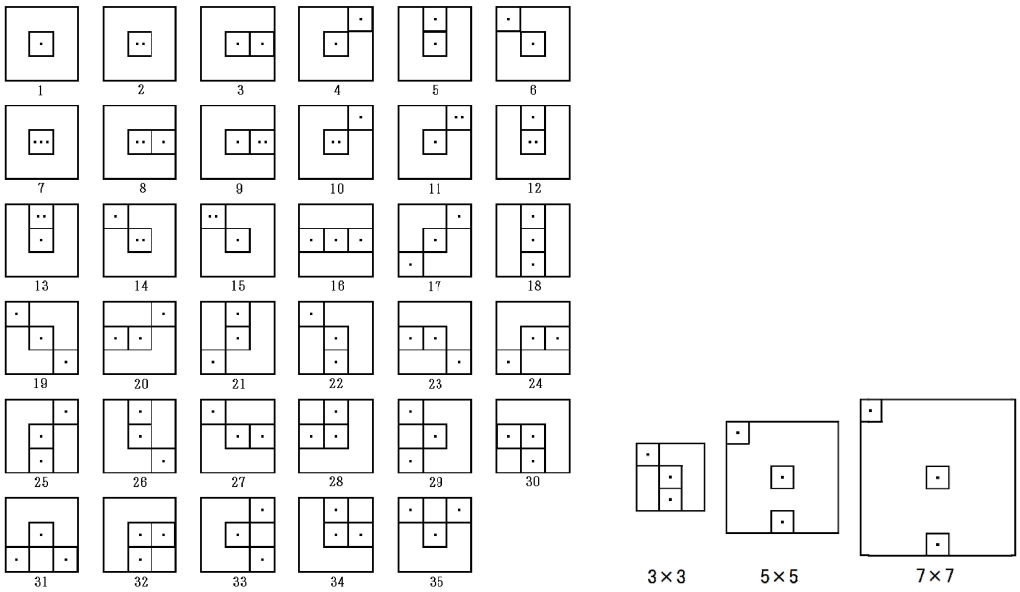

Figure 1. Local mask patterns for HLAC. (a) No.1 is the 0th order, Nos.2 to 6 are the first order, and Nos. 7 to 35 are the second order. (b) Three window sizes of pattern No.22 for HLAC.

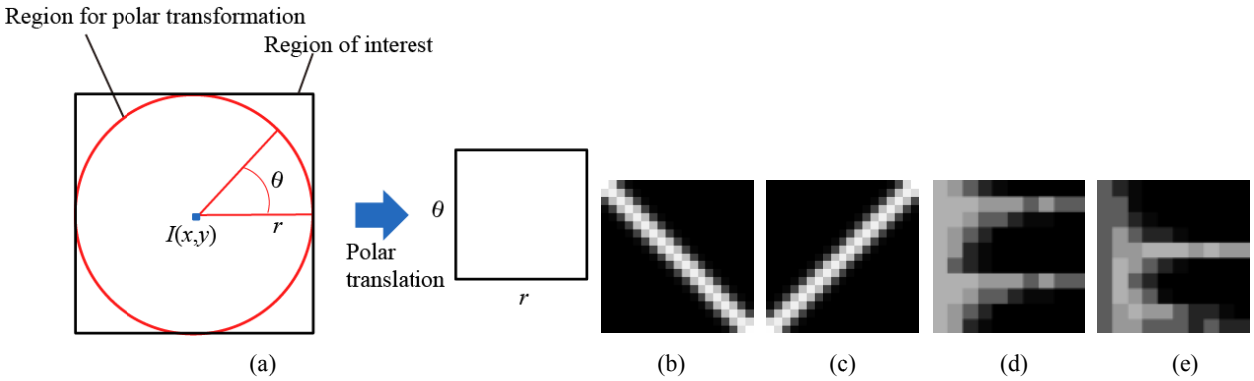

Figure 2. Polar transformation of ROI: (a) polar transformation; (b) and (c) blood vessel models; (d) and (e) polar-transformed images of (b) and (c).

program in the Netherlands and are equally divided into training and testing sets. The images were 565 × 584 pixels and 24 bit color. For each image, manual segmentation result for blood vessels is provided as a reference standard.

2.3 Flow of proposed method

The contrast of blood vessels is highest in the green channel of the color retinal image; thus, a grayscale image was obtained using the green channel. Due to the flash, there is an atypical change in the color of the fundus images. Consequently, the grayscale images were preprocessed using γ-correction and histogram-spreading. The blood vessel regions were enhanced by BTH transformation. A 19 × 19-pixel ROI was set in the BTH image, and ROI was converted to 64 gray levels. To ensure rotation invariance, the ROI was then transformed to a 10 × 10-pixel polar coordinate image. By scanning the retinal images, 105 mask patterns of HLAC features of all pixels were calculated.

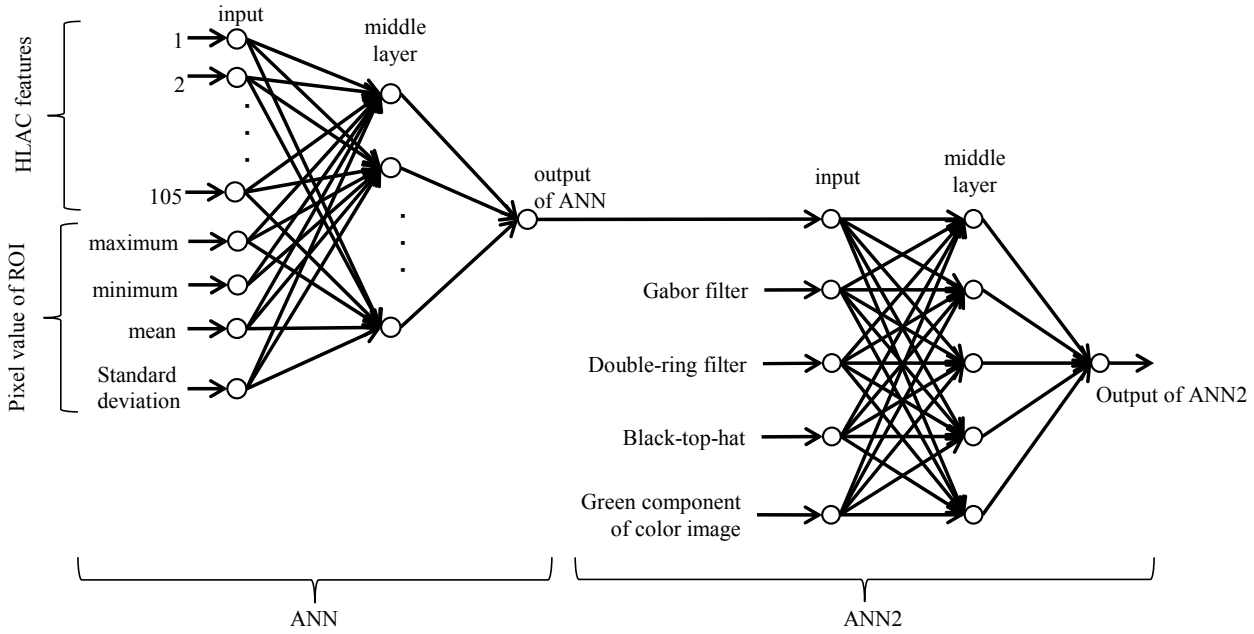

Figure 3. Two artificial neural networks (ANN). First ANN was constructed 12 middle layer units, and it outputs the preliminary blood vessels image. Second ANN (ANN2) was constructed by using 5 middle layer unites, and the final blood vessel image is outputted.

One hundred five HLAC features and four features were input to an artificial neural network (ANN), which is shown in Figure 3. Four features are the maximum value, minimum value, mean and standard deviation of the pixel values in the ROI. A feed forward three-layered network with twelve middle layer units was employed. To complete the training in reasonable time and to reduce the effect of overtraining, the ANN was trained using 10,000 randomly selected samples with the HLAC feature in 20 training images by using a back-propagation algorithm. Each five thousand samples inside and outside of the blood vessel region were selected randomly from each image.

2.4 Comparison with previous methods

HLAC was compared with four methods, i.e., GF, DR filter, and BTH transformation. The GF is calculated as follows:

$$g(x,y) = \exp\left(-\frac{x'^2+\gamma^2 y'^2}{2\sigma^2}\right)\cos\left(2\pi\frac{x'}{\lambda}+\emptyset\right) \quad (2)$$

where

$$x' = x\cos\theta + y\sin\theta$$
$$y' = -x\sin\theta + y\cos\theta \quad (3)$$

In this study, $\lambda = 12$ and $\emptyset = 1$ were determined, and the filtered image used the maximum value of $g(x,y)$ by setting θ = 0, 1/12, 2/12…, 11/12. The DR was then structured from the inner circle and outer ring regions. The radii of the inner circle and outer ring were determined to be 1 and 9 pixels, respectively. The structural element of BTH was also determined to be a circle with a diameter of 7 pixels.

2.5 HLAC combined with four methods

To improve performance, a second ANN (ANN2) with five middle layer units (as shown in Figure 3) classified the blood vessels by using the green component of color image and the four outputs of ANN, GF, DR, and BTH. ANN2 was trained using 10,000 randomly selected samples with outputs from the initial ANN using the same methods.

3. RESULTS AND DISCUSSION

To evaluate the proposed method using HLAC features, 20 test images from the DRIVE database were used. The results were compared with HLAC (ANN), GF, DR, BTH and ANN2. The outputs from all methods were evaluated using the area under the curve (AUC) based on receiver operating characteristics (ROC) analysis. Table 1 summarizes the results. The AUC for ANN2 was the better than them of all our methods.

The blood vessel extraction results for the various methods are shown in Figure 4. The ANN using HLAC output apparent white values in the blood vessel regions (Figure 4(c)) and could extract blood vessels with low contrast. However, the ANN output white values near the outer blood vessel wall; thus, it tended to overestimate the blood vessel regions. Note that GF and BTH also tended to overestimate the blood vessel regions (Figures 4(d) and 4(f)), and DR tended to underestimate blood vessel regions (Figure 4(e)).

High performance of an ANN is not expected when the cross correlation of each input signals is high. Table 2 shows the cross correlations for the images in Figure 4. The cross correlations of HLAC (ANN) and the other methods were not high, although HLAC used the output of BTH. Note that we have presented only preliminary experimental results. For example, the parameters for a combination of GF, DR, and BTH are not considered. Moreover, there are many different ways to apply HLAC. By using log-polar transformation, HLAC features might be able to extract a blood vessel without depending its diameter, although we used a polar transformed image to calculate HLAC features in this study. HLAC features might be able to be applied to various filtered images, as demonstrated in this study. The methods using Gabor filter or wavelet tended to obtain good performances as shown in Table 1. Thus, the performance may be improved by applying HLAC features to Gabor filter or wavelet. We used an ANN as a machine learning technique; however, we did not test a support vector machine, ada-boost, and etc. Therefore, there is possibility that the performance is improved by applying better machine learning technique.

Tabel 1. Comparison of area under the curves (AUCs)

Method	**AUC**
HLAC (Output of ANN)	**0.935**
GF	0.875
DR filter [15]	0.842
BTH transformation [16]	0.918
Green component of color retinal image	0.791
ANN2	**0.960**
Chaudhuri et al. [7]	0.788
Zana et al. [13]	0.898
Muramatsu et al. [17]	0.918
Niemeijer et al. [2]	0.929
Staal et al. [10]	0.952
Ricci et al. [8]	0.956
Soares et al. [3]	0.961
Rangayyan et al. [4]	0.961

Table 2. Cross correlations of images in Figure 4

Method	HLAC		
GF	0.700	GF	
DR	0.555	0.713	DR
BTH	0.688	0.795	0.755

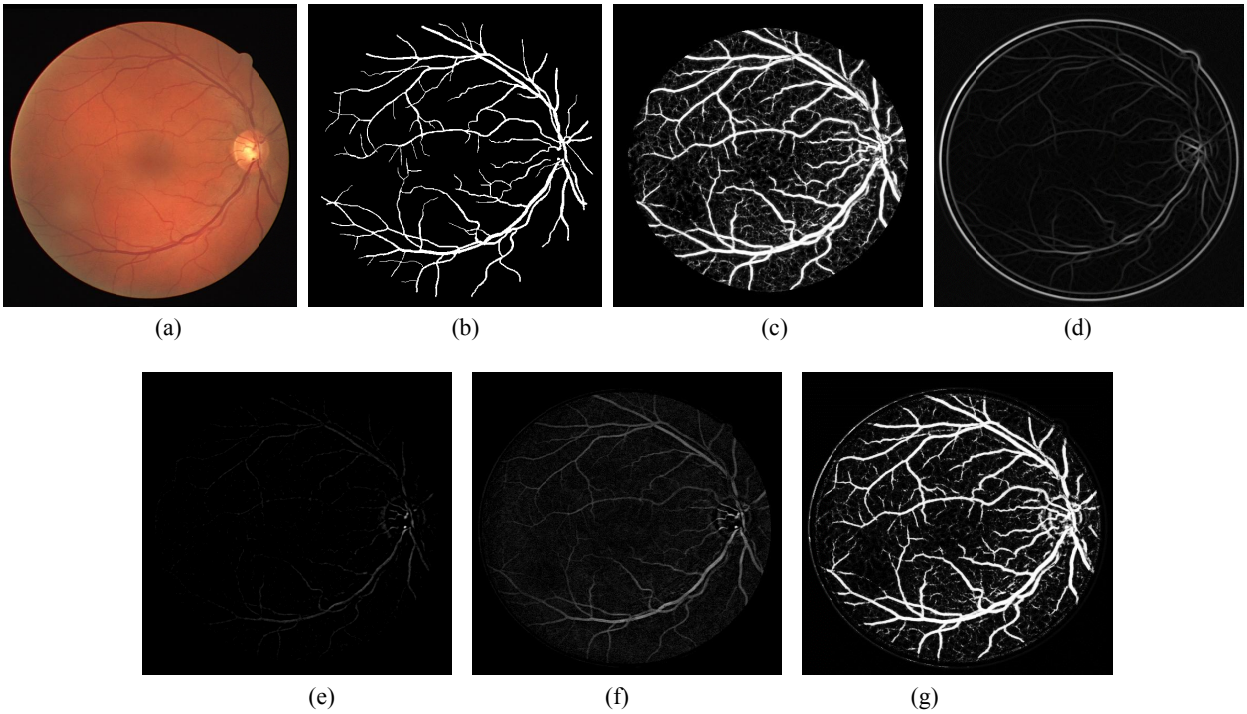

Figure 4. .Examples of blood vessel extraction (image no. 20): (a) original color image; (b) manual segmentation (ground truth); (c) HLAC (ANN); (d) GF; (e) DR filter; (f) BTH transformation; (g) ANN2

4. CONCLUSION

We have proposed a blood vessel extraction method using HLAC features and four features based on an ANN. The AUC of the proposed method reached 0.960 in this study. The proposed method can be useful for automatic blood vessel extraction and is planned to apply the artery-to-vein ratio measurement for help of hypertensive retinopathy. Although it is evident that HLAC can extract blood vessels, many other factors must be considered.

ACKNOWLEDGMENT

This study was supported in part by a grant from Terumo Life Science Foundation in Japan, and a grant for the Grant-in-Aid for Scientific Research on Innovative Areas (Number 26108005) from the Ministry of Education, Culture, Sports, Science and Technology, Japan. The authors are grateful to the co-workers from the University of Shiga Prefecture and Gifu University, Japan.

REFERENCES

[1] Tolias Y. A. and Panas S. M., "A fuzzy vessel tracking algorithm for retinal images Based on Fuzzy Clustering," IEEE Trans. Med. Img. 17(2), 263-273 (1998).

[2] Niemeijer M., Staal J.J., van Ginneken B., Loog M. and Abrámoff, M.D., "Comparative study of retinal vessel segmentation methods on a new publicly available database," Proc. SPIE: Medical Imaging 5370, 648-656 (2004).

[3] Soares J. V. B., Leandro J. J. G., Cesar Jr. R. M., Jelinek H. F. and Cree M. J., "Retinal vessel segmentation using the 2-D Gabor wavelet and supervised classification," IEEE Trans. Med. Img. 25(9), 1214-1222 (2006).

[4] Rangayyan R. M., Ayres F. J., Oloumi F., Oloumi F. and Eshghzadeh-Zanjani P., "Detection of blood vessels in the retina with multiscale Gabor filters," J. Electron. Img. 17(2), 023018 (2008).

[5] Kharghanian R. and Ahmadyfard A., "Retinal blood vessel segmentation using Gabor wavelet and line operator," Int. J. Machine Learning and Computing 2(5), 593-597 (2012).

[6] Miri M. S. and Mahloojifar A., "Retinal image analysis using curvelet transform and multistructure elements morphology by reconstruction," IEEE Trans. Biomed. Eng. 58(5), 1183-1192 (2011).

[7] Chaudhuri S., Chatterjee S., Katz N., Nelson M. and Goldbaum M., "Detection of blood vessels in retinal images using two-dimentional matched filters," IEEE Trans. Med. Img. 8(3), 263-269 (1989).

[8] Ricci E. and Perfetti R., "Retinal blood vessel segmentation using line operator and support vector classification," IEEE Trans. Med. Img. 26(10), 1357-1365 (2007).

[9] Yu G., Li P., Miao Y. L. and Bian Z. Z., "Multiscale active contour model for vessel segmentation," J. Med. Eng. Technol. 32(1), 1-9 (2008).

[10] Staal J. J., Abramoff M. D., Niemeijer M., Viergever M. A. and van Ginneken B., "Ridge based vessel segmentation in color images of the retina," IEEE Trans. Med. Img. 23(4), 501-509 (2004).

[11] Salem S. A., Salem N. M. and Nandi A. K., "Segmentatino of retinal blood vessels using a novel clustering algorithm (RACAL) with a partial supervision strategy," Med. Biol. Eng. Comput. 45(3), 261-273 (2007).

[12] Paripurana S., Chiracharit W., Chamnongthai K. and Saito H., "Extraction of blood vessels in retinal images using resampling high-order background estimation," IEICE Trans. Info. Sys. E98-D(3), 692-703 (2015).

[13] Zana, F. and Klein, J., "Segmentation of vessel-like patterns using mathematical morphology and curvature evaluation," IEEE Trans. Img. Processing 10(7), 1010-1019 (2001).

[14] Hatanaka Y., Nagahata Y., Muramatsu C., Okumura S., Ogohara K., Sawada A., Ishida K., Yamamoto T. and Fujita H., "Improved automated optic cup segmentation based on detection of blood vessel bends in retinal fundus images," Proc. 36th Annu. Int. Conf. IEEE Eng. Med. Biol. Soc., 126-129 (2014).

[15] Hatanaka Y., Nakagawa T., Hayashi Y., Aoyama A., Zhou X., Hara T. and Fujita H., "Automated detection algorithm for arteriolar narrowing on fundus images," Proc. 27th Annu. Int. Conf. IEEE Eng. Med. Biol. Soc., 286-289 (2005).

[16] Nakagawa T., Hayashi Y., Hatanaka Y., Aoyama A., Mizukusa Y., Fujita A., Kakogawa M., Hara T., Fujita H. and Yamamoto T., "Recognition of optic nerve head using blood-vessel-erased image and its application to production of simulated stereogram in computer-aided diagnosis system for retinal images," IEICE Trans. Info. Sys. J89-D(11), 2491-2501 (2006).

[17] Muramatsu, C., Hatanaka, Y., Iwase, T., Hara, T. and Fujita, H., "Automated selection of major arteries and veins for measurement of arteriolar-to-venular diameter ratio on retinal fundus images," Computerized Medical Imaging and Graphics 35(6), 472-480 (2011).

[18] Muramatsu C., Mizukami A., Hatanaka Y., Sawada A., Hara T., Yamamoto T. and Fujita H., "Improvement on recognition of major arteries and veins on retinal fundus images by template matching with vessel models," Medical Imaging and Information Sciences 30(3), 63-69 (2013).

[19] Otsu N. and Kurita T., "A new scheme for practical, flexible and intelligent vision systems," Proc. IAPR Workshop on computer Vision, 431-435 (1988).

[20] Kurita T., Otsu N. and Sato T., "A face recognition method using higher order local autocorrelation and multivariate analysis," Proc. 11th Int. Conf. Pattern Recognition I, 530-533 (1992).

[21] Hara T., Hirose M., Zhou X., Fujita H., Kiryu T., Yokoyama R. and Hoshi H., "Nodule detection in 3D chest CT images using 2nd order autocorrelation features," 27th Annu. Int. Conf. IEEE Eng. Med. Biol. Soc., 6247-6249 (2005).

[22] Okutani D., Hiramoto M. and Maeno K., "Human sensing technique using microwave doppler radar based on higher-order local autocorrelation features," IEICE Technical Report. Speech 113(29), 13-18 (2013).